

Article citation info:

Albaghdadi AM, Baharom M, Sulaiman S. Hybrid methodology using balancing optimization and vibration analysis to suppress vibrations in a double crank-rocker engine. *Eksploracja i Niezawodność – Maintenance and Reliability* 2022; 24 (1): 53–61, <http://doi.org/10.17531/ein.2022.1.7>.

Hybrid methodology using balancing optimization and vibration analysis to suppress vibrations in a double crank-rocker engine



Anwr M. Albaghdadi^{a,*}, Masri Baharom^a, Shaharin Sulaiman^a

^aUniversiti Teknologi Petronas (UTP), Department of Mechanical Engineering, 32610 Bandar Seri Iskandar, Perak, Malaysia

Highlights

- A combination of balancing and vibration analysis is introduced for engine evaluation.
- Variable speed balancing optimization was conducted for reliable results within speed range.
- Vibration analysis was performed in frequency and time domain for comparison and verification.
- Vibration analysis operates as a monitoring tool for engine balancing process outcome.

Abstract

This study aims to present mathematical modelling to evaluate and analyze double crank-rocker engine performance. The study suggests the use of two methods to reduce system vibration through balancing optimization and vibrational analysis. The combination of both methods acts as a verification method; besides it can be used as a tool for further system design enhancement and condition monitoring. The derived mathematical model is then used for balancing optimization to identify system shaking forces and moments, while variable speed is considered as an added parameter to evolve the optimization process. This factor shows better enhancement in reducing system shaking forces and moments compared to constant speed balancing method. Next, the system characteristics were concluded in terms of mode shapes and natural frequencies using modal and frequency response analysis, which give clear clue for secure system operational ground. Finally, the reduction in system vibrations was translated into engine's centre of mass velocity, which evaluates balancing process effectiveness and indicate if further enhancement should be conducted.

Keywords

This is an open access article under the CC BY license (<https://creativecommons.org/licenses/by/4.0/>)

balancing optimization, vibration analysis, double crank rocker engine, mathematical modelling, and simulation.

1. Introduction

Internal combustion engines are still the most dominant engines in today's transportation and power generation aspects. Therefore, development and condition monitoring of these engines are crucial to achieve better efficiency, higher safety, and more reliable for users. Vibrations resulted from these engines are considered as one of the biggest issues that degrade overall performance. Hence, vibration reduction is a key factor to elevate these machines productivity level and to monitor their endurance during desired working period. Vibration monitoring and analysis is one of the best tools that enable researchers and engineers to understand various problems accompanied by these engines [20].

Recently, the crank-rocker engine was introduced as a newly invented engine, where high-performance outcome was achieved due to its unique configuration [13]. However, as any new engine, this engine is still under continuous enhancement process to receive better outcome in terms of thermal and mechanical performances. This new configuration is found to have a vibration problem which might lead to degradation of engine overall performance. In this particular case, vibration was mainly caused by mechanism unbalance which led to system high shaking forces and moments. To overcome vibration issue, proper dynamic study and balancing must be done, then a

system performance study would prove the efficiency of this process. Therefore, in his research, Mohammed et.al. [12] proposed a method to reduce resulting forces caused by system unbalance. This study succeeded in eliminating all shaking forces by adding counterweights to both crank and rocker linkages. but, shaking moments are naturally accompanying counterweights added as a trade-off when using such method [4]. Hence, the need for new methods to eliminate both shaking forces and shaking moments are required, and some of these methods were discussed previously in [2]. The suggested configuration is using a duplicate crank-rocker mechanism arrangement to counter the inertial forces caused by this mechanism. Based on previous studies, a reliable vibration investigation is needed to investigate the outcome from balancing process and validate the suggested method. Hence, in this study, a vibrational study is introduced to explore the transmitted vibration levels from this mechanism configuration to the engine block during operating conditions.

The purpose of recognizing the vibration problem and identifying all excitations forces, is to create a proper tool that can be utilized to analyse and troubleshoot these machines. Delvecchio et. al. [6] introduced literature on different methods used to analyze and perform a condition monitoring tool that can be used practically on internal combustion engines. Different fault conditions caused by engine vi-

(*) Corresponding author.

E-mail addresses: AM. Albaghdadi (ORCID: 0000-0003-2680-419X): al.bghdady@gmail.com, M. Baharom (ORCID: 0000-0001-9437-9186): masrib@utp.edu.my, S. Sulaiman (ORCID: 0000-0001-8819-6703): shaharin@utp.edu.my

brations were identified then diagnostic techniques and applications were discussed accordingly. In their study, Hmida et. al. [8] discussed some factors that cause engine vibrations such as combustion pressure, inertial and torsional forces, misalignment and engine main structure, etc. with the emphasis on problems accompanying cyclic variations and misfiring in engine. The authors suggested a mathematical model to analyze the effects of misfiring on crankshaft vibrations. Likewise, Liu et. al. [10] introduced piston slap of a reciprocating engine as the biggest source of vibration. In their simulation, he noticed the importance of including the torsional forces of single-cylinder reciprocating system analysis to estimate the overall vibration.

As for measuring and identifying internal combustion engine excitation forces and their impact, Zhao et. al. [23] identified and measured the excitation forces of 2-cylinder diesel engine besides combustion pressure which are cylinder slap, bearing load and inertial forces. The author claimed that the acquired data can be used effectively to model this engine, and to be used to eliminate non-combustion excitation forces. Zhao et. al. [22] suggested an inverse method to find these forces from the measured velocity of engine mounting points. This method was found to be effective to reconstruct the exact values of forces and moments values. A similar approach was proposed by [19] using the interpolation method to establish engine excitation forces.

Generally, vibration could be suppressed practically by eliminating the source causing these vibrations, such as applying balancing [7] or alignment [1] to rectify equipment problems. Another method is by isolating the vibratory element from the rest of the system by applying isolators such as mechanical shock dampeners, mechanical or hydraulic absorbers, or both depending on design aspects [17]. Another classification of vibration reduction methods are also presented as passive, semi-active and active methods [3]. Wang et. al. [18] presented three methods to isolate the vibrations of a vehicle during engine start-stop operation. All three methods concluded that increasing mounting damping coefficient is more efficient to reduce these vibrations. Similarly, Ooi et. al. [14] perform an optimization process to determine engine mounts stiffness and location. The optimized values show less force transmission from engine block to the ground compared to original engine configuration. Similar work for vibration isolation and control in high speed, heavy-duty engines was introduced in [21], also by using active mount system in [9]. In their research, Slesongsom et. al. [16], introduced a new design method through part shape design optimization to overcome vibrations on a single-cylinder engine. This process resulted an optimal design of the shape of the moving part which is considered practical to control parts vibration amplitudes. More approaches and techniques were introduced in [11] for vibration reduction in the application of internal combustion engine.

Usually, the balancing process is used to overcome shaking forces and moments of specific mechanism configuration, but when this mechanism is integrated into a mechanical system, vibration might still present due to parameters interference such as system masses, stiffness and damping of different elements. In practice, Tuning and testing the system vibrations after performing balancing might take a lot of effort and time. Therefore, this paper intends to introduce a combined study on balancing optimization and vibration analysis for double crank-rocker (DCR) engine design enhancement and as a future troubleshooting tool. The advised model is desired to introduce a basic tool to identify pre- and post-balanced engine excitation forces, analyze the system and predict engine performance. The construction of this paper goes through 6 DOF mathematical modelling of this engine model, which leads to the identification of the excitation forces caused by shaking forces and moments resulted from this mechanism operation. Next, the method of conducting balancing optimization is proposed, followed by modal and vibrational analysis of this system. The results and discussion are presented by performing a comparison between virtual engine model dynamic response and simulation results of this engine model, with verification.

2. Methodology and mathematical model

2.1. Six DOF DCR engine dynamic model

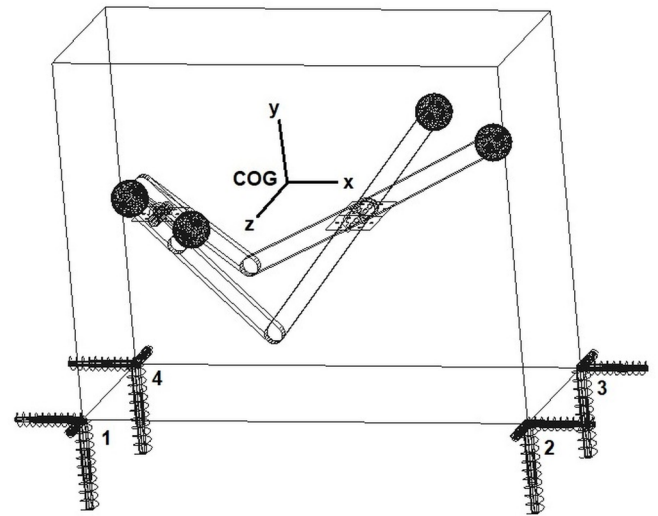


Fig. 1. DCR mechanism and engine block

In this section, the equation of motion of DCR engine model is constructed, as illustrated in Figure (1). This engine block is considered to have six degrees of freedom, also is treated as a rigid body. The engine model is attached to the ground via twelve dampers fixed into four points and oriented in three directions, namely X, Y and Z. The equation of motion for this engine can be described as:

$$M\ddot{X}(t) + C\dot{X}(t) + KX(t) = F(t) \quad (1)$$

where M , C and K represent engine block mass, damping and stiffness of each spring, introduced by 6x6 matrices. X , \dot{X} , and \ddot{X} are displacement, velocity, and acceleration of the system respectively. $F(t)$ is the excitation forces applied on the system. The matrix of engine mass M can be represented by:

$$M = \begin{bmatrix} m & 0 & 0 & 0 & 0 & 0 \\ 0 & m & 0 & 0 & 0 & 0 \\ 0 & 0 & m & 0 & 0 & 0 \\ 0 & 0 & 0 & I_{xx} & -I_{xy} & -I_{xz} \\ 0 & 0 & 0 & -I_{xy} & I_{yy} & -I_{yz} \\ 0 & 0 & 0 & -I_{xz} & -I_{yz} & I_{zz} \end{bmatrix} \quad (2)$$

Where x , y , and z are the centre of gravity (COG) location of engine mass and coincide with system global coordinate position. Additionally, engine block moments of inertia with respect to the origin of the global coordinate system are referred by I_{xx} , I_{yy} and I_{zz} . Matrices of the stiffness and damping, are introduced by:

$$k_i = \begin{bmatrix} k_{ix} & 0 & 0 \\ 0 & k_{iy} & 0 \\ 0 & 0 & k_{iz} \end{bmatrix} \quad (3)$$

$$c_i = \begin{bmatrix} c_{ix} & 0 & 0 \\ 0 & c_{iy} & 0 \\ 0 & 0 & c_{iz} \end{bmatrix} \quad (4)$$

where k_i , and c_i represents each individual mounting i , stiffness and damping position corresponding to local location ($ix, iy, and iz$), where $i=1, 2, 3$ and 4. To transfer both matrices from the local to the global coordinate position, a 3×3 transformation matrix A is needed. This matrix is identified using the Euler angle matrix [14], which is represented by:

$$[A] = \begin{bmatrix} \cos \alpha \cos \gamma & -\sin \alpha \cos \beta + \cos \alpha \sin \gamma \sin \beta & \sin \alpha \sin \beta + \cos \alpha \sin \gamma \cos \beta \\ \sin \alpha \cos \gamma & \cos \alpha \cos \beta + \sin \alpha \sin \gamma \sin \beta & -\cos \alpha \sin \beta + \sin \alpha \sin \gamma \cos \beta \\ -\sin \gamma & \cos \gamma \sin \beta & \cos \gamma \cos \beta \end{bmatrix} \quad (5)$$

where α, β and γ are rotation angles about the X-, Y- and Z-axes respectively. Hence, the transformed matrices of stiffness and damping can be calculated by:

$$k = A^{-1} k_i A \quad (6)$$

and:

$$c = A^{-1} c_i A \quad (7)$$

where k and c are the coefficient stiffness and damping matrices in the global coordinates. As for the excitation forces, it can be formulated by 6×1 vector as follows:

$$F = \begin{Bmatrix} F_x \\ F_y \\ F_z \\ T_x \\ T_y \\ T_z \end{Bmatrix} \quad (8)$$

where F represents shaking forces component in the relevant coordinate, and T is the shaking moment component about the corresponding axis. More details on identifying the excitation forces are discussed in the next section. The displacement vector is composed of 6×1 matrix as follows:

$$X = \begin{Bmatrix} \delta_x \\ \delta_y \\ \delta_z \\ \theta_x \\ \theta_y \\ \theta_z \end{Bmatrix} \quad (9)$$

where δ and θ represent COG transitional and angular displacement vector of engine respectively corresponding to the relevant axis.

2.2. Excitation forces identification

Forces generated during internal combustion engine operation result from many reasons such as combustion pressure, engine internal parts friction, interconnection with other equipment, and speed fluctuation. In this section, forces produced by DCR parts inertial forces are highlighted to investigate the suggested mechanism stability and to make sure this engine can be elevated to the next design level. Previously, several studies were conducted to perform balancing on this mechanism [2], the advised model has shown a significant reduction in both shaking forces and moments. When this mechanism is desired

to be integrated into the developed engine assembly, a vibrational analysis would help to identify engine design parameters such as corresponding masses, dampers, and stiffness characteristics. Furthermore, it is desirable to tune the whole system vibrations, identify safe operating conditions and avoid any probable damages which might occur during engine lifespan.

The transmitted forces due to mechanism inertial forces to the supporting engine bearings can be calculated using virtual work method which was illustrated in precedent studies. The generated forces are measured on joints connecting engine mechanism and engine block, which represents bearing housing in practice. The force-measurements corresponding to their axes of action are theoretically represented by:

$$\bar{F}_x = F_{C2x} + F_{R1x} - (F_{C1x} + F_{R2x}) \quad (10)$$

$$\bar{F}_y = F_{C1y} + F_{R2y} - (F_{R1y} + F_{C2y}) \quad (11)$$

$$\bar{F}_z = F_{C1z} + F_{R2z} - (F_{R1z} + F_{C2z}) \quad (12)$$

$$\bar{F} = \sum (\bar{F}_x^2 + \bar{F}_y^2 + \bar{F}_z^2)^{\frac{1}{2}} \quad (13)$$

where \bar{F} is the summation of generated forces \bar{F}_x , \bar{F}_y , and \bar{F}_z , on the linking joints with respect to X_i , Y_i and Z_i coordinates. These forces are generated from the crank shaking forces F_C and rocker forces F_R for the same coordinate system, where two pairs of crank linkages $C_{1,2}$ and rocker linkages $R_{1,2}$ are involved. Similarly, the exerted moments of this mechanism about relevant axes are illustrated by:

$$\bar{T}_x = \frac{P_1}{2} \times (F_{R1y} + F_{R2y} - F_{C1y} - F_{C2y}) \quad (14)$$

$$\bar{T}_y = \frac{P_1}{2} \times (F_{C1x} + F_{C2x} - F_{R1x} - F_{R2x}) \quad (15)$$

$$\bar{T}_z = \frac{P_2}{2} \times (F_{C1y} - F_{C2y} + F_{R1y} - F_{R2y}) \quad (16)$$

$$\bar{T} = \sum (\bar{T}_x^2 + \bar{T}_y^2 + \bar{T}_z^2)^{\frac{1}{2}} \quad (17)$$

where \bar{T} is the total moment of shaking moments \bar{T}_x , \bar{T}_y , and \bar{T}_z , caused by parts inertial forces about relevant axes. P_1 is the space between both linkages, and P_2 is the distance between fixed joints. The resulting forces and moments are calculated in the local coordinate system and need to be transferred to the global coordinate system using the transformation matrix A used in (7) as follows:

$$F = [A]^{-1} * \begin{Bmatrix} \bar{F} \\ \bar{T} \end{Bmatrix} \quad (18)$$

The above matrix is expected to have a periodic but non-harmonic time wave-form of the acting forces, owing to the interaction between double mechanism arrangement.

2.3. Frequency response function and modal analysis

If we consider a system under multiple excitation forces as input and multiple outputs, an analysis of a multi-degree of freedom MDOF system response can be translated using analysis of a group of single

degree of freedom (SDOF). The conceptual representation for this solution is illustrated in Figure (2). This indicates that implementing a superposition approach can correlate final output response to related input forces.

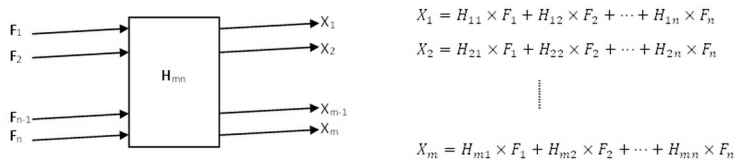


Fig. 2. Response representation of a system for multiple inputs and multiple outputs

Hence, each individual SDOF can be described in terms of natural frequency ω_n and damping ratio ξ , where both can be found by:

$$\omega_n = \sqrt{\frac{k}{m}} \quad (19)$$

$$\xi = \frac{c}{2\sqrt{km}} \quad (20)$$

The solution for the dynamic equation can be assumed to be:

$$F(t) = F_0 e^{i\omega t} \quad (21)$$

$$X(t) = X_0 e^{i\omega t} \quad (22)$$

where ω is the excitation frequency, F_0 and X_0 are the force and displacement amplitudes respectively at the respective frequency. The corresponding derivative to displacement give us velocity and acceleration equation as follows:

$$\dot{X}(t) = i\omega X_0 e^{i\omega t} \quad (23)$$

$$\ddot{X}(t) = -\omega^2 X_0 e^{i\omega t} \quad (24)$$

Apply equations (19)-(21) to the solution to SDOF system dynamic equation represented in (1) gives us displacement response as follows:

$$X = \frac{\delta}{\sqrt{(1-r^2)^2 + (2\xi r)^2}} \quad (25)$$

$$\varnothing = \tan^{-1} \frac{2\xi r}{1-r^2} \quad (26)$$

It can be noticed that the response is complex where X is the amplitude and \varnothing is the response lag of the excitation frequency. The terms δ and r , are the static displacement and excitation frequency of natural frequency ratio respectively and are identified by:

$$\delta = \frac{F_0}{k} \quad (27)$$

$$r = \frac{\omega}{\omega_n} \quad (28)$$

Moreover, when considering the relation between outputs to inputs in frequency domain, the magnitude H_ω is calculated using the frequency response function (FRF) represented by:

$$H_\omega = \frac{\text{Output}}{\text{Input}} = \frac{X_\omega}{F_\omega} \quad (29)$$

Practically, to determine FRF of such system measurements, the procedure is performed by utilizing the spectra of output vibration response to the input force amplitudes. This can be achieved easily using Fast Fourier Transform (FFT) method.

In this study, the flow of the vibration analysis is performed through these steps:

- Identify system dynamic governing equations to correlate inputs to the outputs.
- Introduce modal analysis to identify system natural frequencies and corresponding shape modes.
- Find the response of the system according to the applied system forces.

Representation of FRF and system response usually can be introduced using one of three measurements, namely receptance identified by displacement X , mobility identified by velocity \dot{X} , or inertance defined by acceleration \ddot{X} , where each is in relation to the input excitation forces F . In this paper, the adopted measurement of the output response is to find system mobility, and this is justified since the frequency range is in the middle range i.e., 10 to 1000 Hz as per ISO 10816. This measurement handling is considered a good practice when dealing with applications such as rotating equipments and internal combustion engine [5].

2.4. Balancing optimization method

This part introduces balancing method conducted to determine the counterweights to be attached to the DCR mechanism to reduce resulting shaking forces and shaking moments. The basic steps considered to perform this optimization are firstly using mechanism kinematics and dynamics analysis to identify system constraints, then to decide on the design variables, and lastly to implement the objective function from equations derived in the previous section.

Usually, mechanism balancing studies are conducted at a constant speed (CS) when performing optimization of working mechanism, and seldom researches were observed to conduct variable speed (VS) balancing for less vibration values [15]. In this study, it is desired to include variable speed as a crucial factor to perform balancing optimization, which is more adequate and reasonable for implementing this mechanism in internal combustion engine applications. This enhanced approach is expected to present better engine stability within engine working speed range. This engine is desired to work under variable speed from 0 to 5000 rpm, and frequency range will be taken from 0 to 100 Hz for this study analysis. The DCR engine configurations are stated in Table (1).

It is suggested to use counterweights to balance this engine mechanism for simplicity, so four counterweights are attached to the crank and rocker linkages, and their masses are taken as design variables μ_j for ($j= 1$ to 4). The objective function (of) is introduced using both equations (10) and (14) to achieve the minimum shaking forces and moments resulting during mechanism operation. The optimization function can be written as:

$$of : \text{minimize } (\sigma_1 \bar{F} + \sigma_2 \bar{T}) \quad (30)$$

where σ_1 and σ_2 are weight factors, assigned the values of (0.5, 0.5) respectively. The proposed method is conducted first when engine is experiencing speed variation (VS) during the optimization. The speed

Table 1. DCR engine model configuration

Parameter	values
Engine mass m	30.5 (kg)
Center of gravity, COG location	$[0, 0, 0]^T$ (mm)
Moment of inertia $[I_{xx} I_{yy} I_{zz} I_{xy} I_{yz} I_{zx}]$	$[1.2, 0.88, 0.64, 0, 0, 0] \text{ E}+08$ (Kg.mm ²)
Mount stiffness, k	1900 (newton/mm)
Mount Damping, c	0.1 (newton-sec/mm)
Crank Length $C_{1,2}$	141.4 (mm)
Connecting Rod Length, CR	282.8 (mm)
Rocker length, $R_{1,2}$	640.3 (mm)
Space between linkages, P_1	100 (mm)
Distance between fixation joints, P_1	450 (mm)

during simulation time t is governed by the following conditional equation:

$$VS = \begin{cases} Max\ rpm \times t & \text{if } time < t \\ Max\ rpm & \text{if } time \geq t \end{cases} \quad (31)$$

Then, another optimization is conducted when the engine is running at constant speed CS, (i.e., 2000 rpm), and the maximum speed is 5000 rpm. The outcome results are compared corresponding to the reduction that occurred in the RMS values of system shaking forces and moments. Counterweight (μ_j) masses before and after this optimization operation are listed in Table (2).

3. Results and discussion

In this section, three main subsections are introduced to illustrate the outcomes resulting from the proposed modelling and simulation methods. The first section presents balancing results, where the shaking forces and moments values outcomes are presented and conclude the effectiveness of the utilized balancing method discussed in section 2.4.

Table 3. Shaking forces and moments values with respect to VS and CS balancing method

Simulation rotation speed		Fx (Newton)	Fy (Newton)	Fz (Newton)	Tx (Newton-mm)	Ty (Newton-mm)	Tz (Newton-mm)
0-5000 rpm	CS Balancing (RMS)	1.87E+03	1.95E+03	7.50E-13	8.80E+05	1.30E+06	1.30E+06
	VS Balancing (RMS)	3.24E+02	5.55E+02	4.10E-13	7.50E+05	1.10E+06	2.50E+05
	Diff. %	82.70	71.53	45.33	14.77	15.38	80.77
2000 rpm	CS Balancing (RMS)	6.66E+02	7.09E+02	2.60E-13	3.20E+05	4.40E+05	4.60E+05
	VS Balancing (RMS)	1.16E+02	2.54E+02	1.50E-13	2.70E+05	3.80E+05	8.78E+04
	Diff. %	82.57	64.12	42.31	15.63	13.64	80.92

Table 4. VS and CS simulation results using configurations by VS balancing method

	Engine speed CS @ 2000 rpm			Engine speed VS 0 to 5000 rpm		
	Balanced	Unbalanced	Reduction %	Balanced	Unbalanced	Reduction %
Fx	1.16E+02	2.36E+03	95.09	3.24E+02	6.66E+03	95.14
Fy	2.54E+02	1.59E+03	83.97	5.55E+02	4.40E+03	87.38
Fz	1.40E-13	3.20E-12	95.63	4.13E-13	9.08E-12	95.45
Tx	2.70E+05	4.30E+05	37.21	7.58E+05	1.22E+06	37.87
Ty	3.70E+05	5.90E+05	37.29	1.06E+06	1.68E+06	36.90
Tz	8.78E+04	3.13E+06	97.20	2.46E+05	8.80E+06	97.20

Table 2. Counterweights values

Counter-weight (μ)	Lower limit (Kg)	Initial value (Kg)	Upper limit (Kg)	Optimized value (Kg)	
				VS Balancing	CS Balancing
1	0.01	2	10	2.269	0.01
2	0.01	2	10	2.237	1.32
3	0.01	2	10	0.795	0.876
4	0.01	2	10	0.575	0.902

Then, a modal study is presented where the natural frequencies and corresponding modal shapes of DCR system are established. This will give us an indication of safe operational frequencies and help in further system enhancement. The last part correlates balancing optimized results to perform system mobility response, where engine's COG velocity components are measured and analysed. A comparison between dynamic virtual model and simulation is conducted for results verification.

3.1. Balancing results

The balancing method illustrated in section 2.4 was conducted using the objective function described in equation (16), where the simulation is carried out under two cases: first for variable rotational speed VS of DCR mechanism from 0 to 5000 rpm, and second under constant speed CS of 2000 rpm. The counterweights μ_j are obtained for each case as stated in Table (3), and the results are individually used to perform system dynamic analysis to show the difference between both outcomes

VS balancing optimization method shows better results than CS balancing optimization method in terms of reducing forces and moments exerted by DCR mechanism. The RMS results from both balancing simulations along with percentage difference between both values are listed in Table (3). The difference in percentage was calculated using the following correlation:

$$Diff \% = \frac{CS\ RMS - VS\ RMS}{CS\ RMS} \times 100 \quad (32)$$

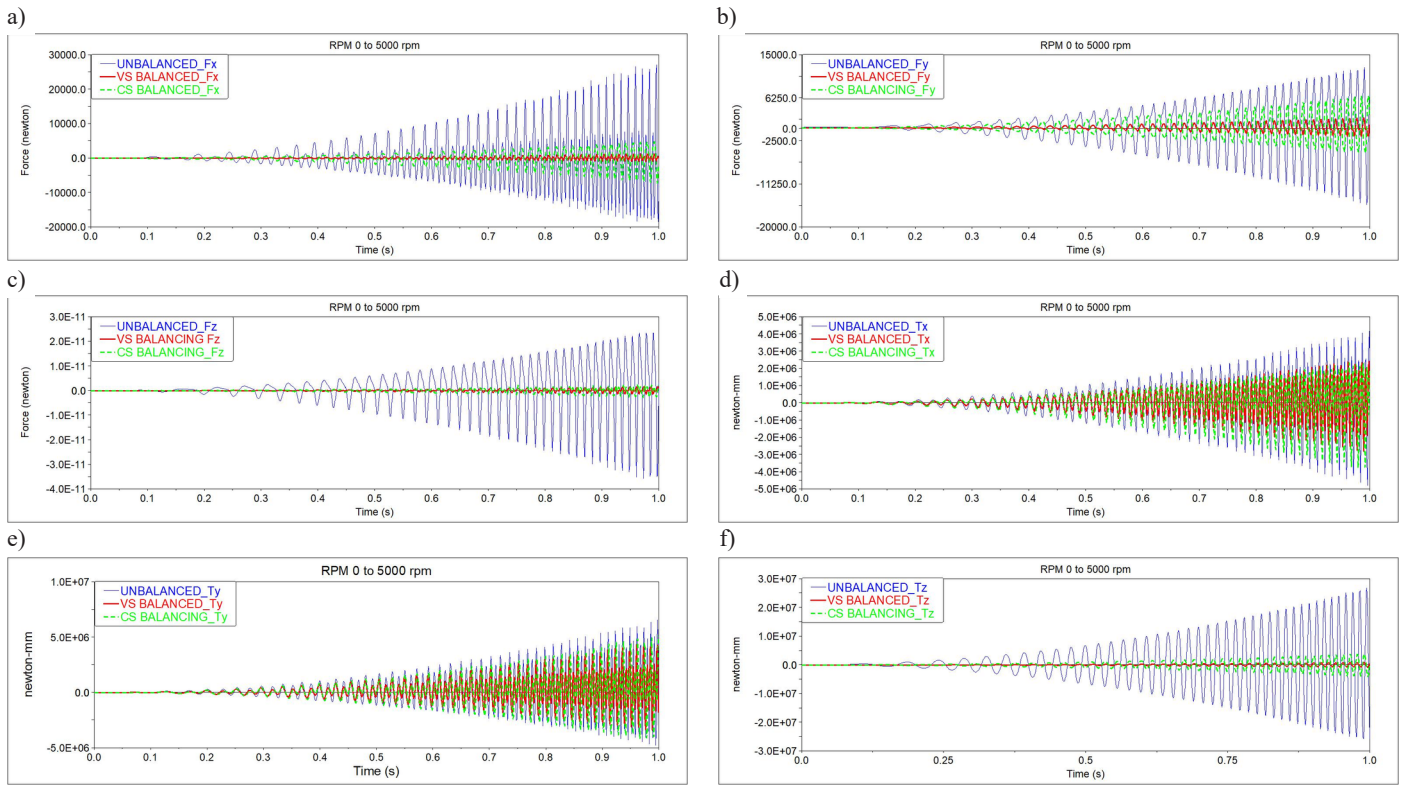


Fig. 3. Engine shaking forces and moments simulation results at variable rotational speed (i.e., 0-5000 rpm), a) Fx, b) Fy, c) Fz, d) Tx, e) Ty, and f) Tz

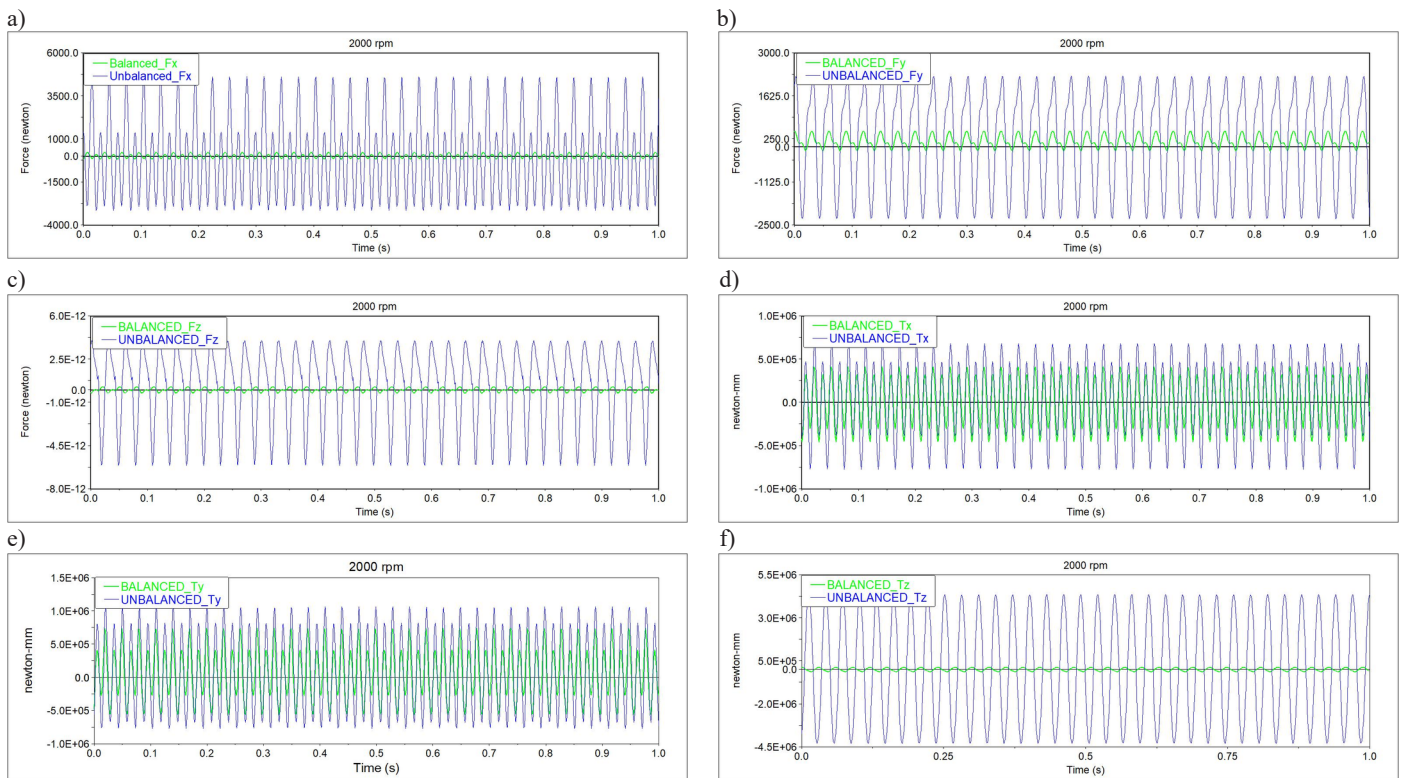


Fig. 4. Engine shaking forces and moments simulation results at constant rotational speed (i.e., 2000 rpm), a) Fx, b) Fy, c) Fz, d) Tx, e) Ty, and f) Tz

For better illustration, Figure (3) illustrates the reduction of system vibrations when simulating the engine under variable speed during simulation time using equation (17). Similarly, Figure (4) represents the outcome of this method if used during constant rotation speed (i.e., 2000 rpm). Table (4) lists the RMS values for vibration results when engine is operated under VS and CS, then compare these results to the unbalanced condition to show reduction percentage. The results of VS balancing method shaking forces and moments are then imple-

mented next in the analysis for further system investigation through vibrational analysis.

3.2. Modal modes and frequency response function analysis

Before carrying out the proposed method to system frequency response analysis, system modal parameters namely natural frequen-

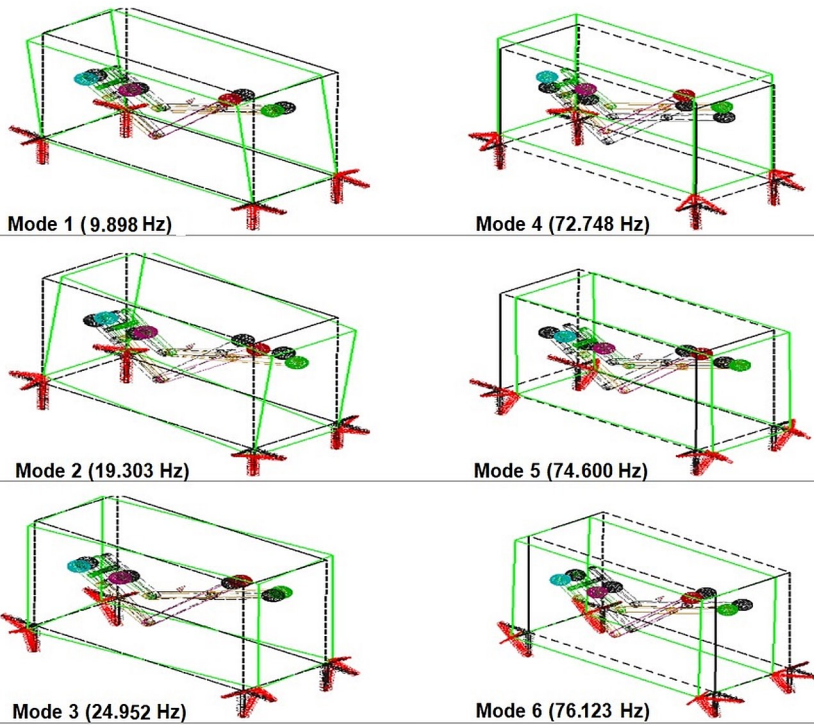


Fig. 5. DCR engine six mode of shapes and corresponding natural frequencies, (dashed lines-original position and solid line-engine mode).

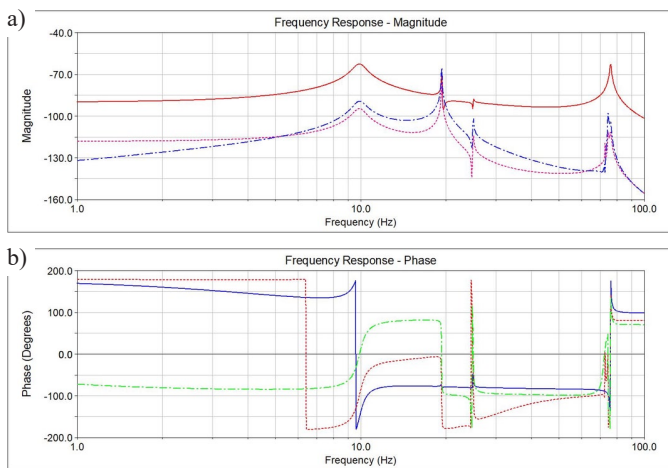


Fig. 6. Model mobility frequency response a) Magnitude and b) Phase

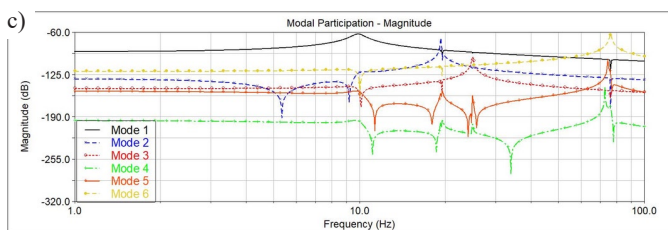


Fig. 7. Individual mode participation for mobility response Y_x

cies and mode shapes are obtained for better visualization and data verification. This test also enables the created model to predict system performance better in case of any modification in the system construction. The modal analysis results using FEM describe DCR frame system free vibration analysis, where a harmonic sinusoidal force of (10 Newton) was applied to excite this system. The mode shapes corresponding to 6-DOF natural frequencies are shown in Figure (5). The illustration presents DCR engine frame mode shapes at their corresponding frequencies in green line, compared to the original position

represented by dashed line. Six shapes plying harmonic forces on this 6 DOF-system, which gives an indication of system behaviour when experiencing one of these operational frequencies.

Since frequency response function has the advantage to include the effects of modes outside the measurement range and the collected data can be set to the desired range of working frequency, the frequency response of DCR mechanism was performed. For result comparison, frequency response for mobility magnitude and phase in decibels are illustrated in Figure (6).

In Figure (6), mobility response in three directions Y_x , Y_y , and Y_z are illustrated in magnitude and phase. System mobility at operational range from 0 to 100 Hz is predicted to indicate critical frequencies that cause higher vibrational values. It can be noted that the frequency recorded for peak responses shows close values to frequencies resulting from modal analysis.

Modes' participation magnitudes are also illustrated in Figure (7), where mobility response Y_x is presented. This shows how each mode contributes to the overall peak frequencies, where six modes are contributing to the mobility response Y_x . Since all modes are participating to a certain degree to determine system response, it can be noticed that frequency response of all mobility outputs is resulted due

to this contribution. For better illustration, Table (5) shows a list of frequency values from both modal and FRF analysis.

3.3. Engine response verification

Due to the change in operating conditions, the relation between system velocity response and excitations are proportional. The reduc-

Table 5. System Natural Frequencies

Frequency Hz	1	2	3	4	5	6
Modal analysis	9.898	19.303	24.952	72.748	74.600	76.123
FRF	9.908	19.319	25.003	72.778	74.473	76.207

tion of input forces is crucial to improve the engine response and to reduce the vibration levels. Figure (8) shows the effect of VS force balancing method illustrated earlier on system velocity response. The resultant forces on the DCR engine block from both CS and VS are reduced and the velocities as well. This gives us indications of how much vibrations can be controlled using this method and how much this system needs to be further enhanced. The simulation speed in this analysis is conducted at 0 to 5000 rpm variable speed, then steady-state after $t=1$ with 5000 rpm. The velocity components Y_x , Y_y , and Y_z show less response by about 80%, 93%, and 22% respectively. Both Y_x , and Y_y shows high reduction in values which is convenient since both are dominant if compared to Y_z , which shows less velocity amplitudes.

The response resulting from VS optimization was verified by comparing between virtual model operated at 2000 rpm and Simulation analysis, see Figure (9). The outcome results for velocity components show almost identical values, where the difference in values for Y_x was about 2.91%, for Y_y was about 4.78%, and for Y_z was about 0.26%. This shows the consistency between proper balancing optimization using VS balancing method and vibration response for DCR engine.

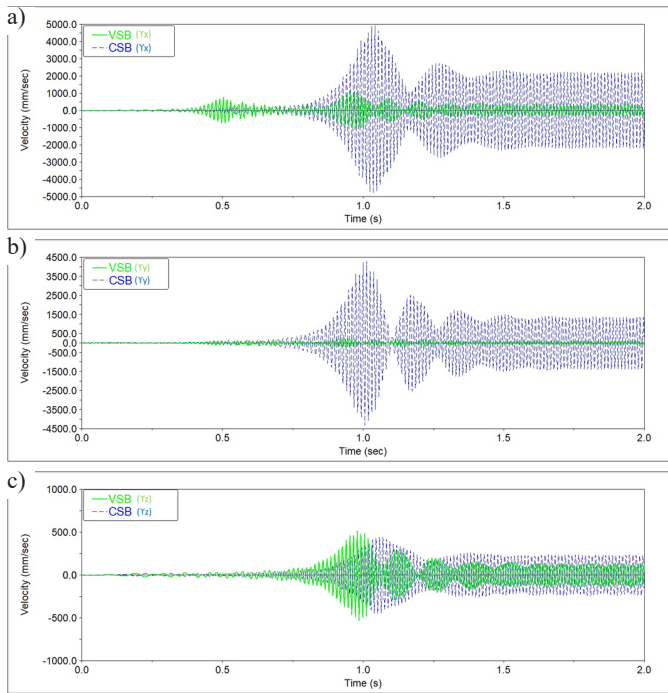


Fig. 8. Velocity response comparison between VS and CS balancing method a) Y_x , b) Y_y , and c) Y_z

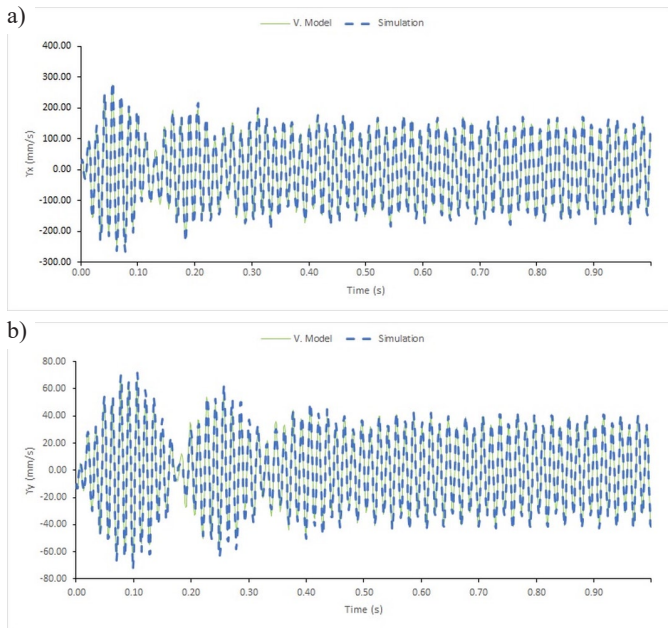


Fig. 9. Velocity response comparison between virtual model and simulation analysis a) Y_x , b) Y_y , and c) Y_z

FFT results for velocity component is introduced in Figure (10) to identify velocity amplitudes corresponding to their frequencies. It is observed that each component is having single or multiple frequencies where it coincides with system natural frequencies identified earlier or coincides with excitation forces frequencies which are in this case having 33.33 and 66.66 Hz, respectively. Moreover, beat phenomena can be identified for Y_x and Y_y in this case owing to the closeness between the forces excitation frequency and system natural frequency values. Another result can be illustrated in figure (11), where resonance occurred in one or more of the velocity components (e.g., Y_x), when the system is excited close enough to the system natural frequency (i.e., 75 Hz). This demonstration shows that if operational frequency matches or gets close to one of the natural frequencies, the system will experience higher vibration levels, which should be considered during design and operations.

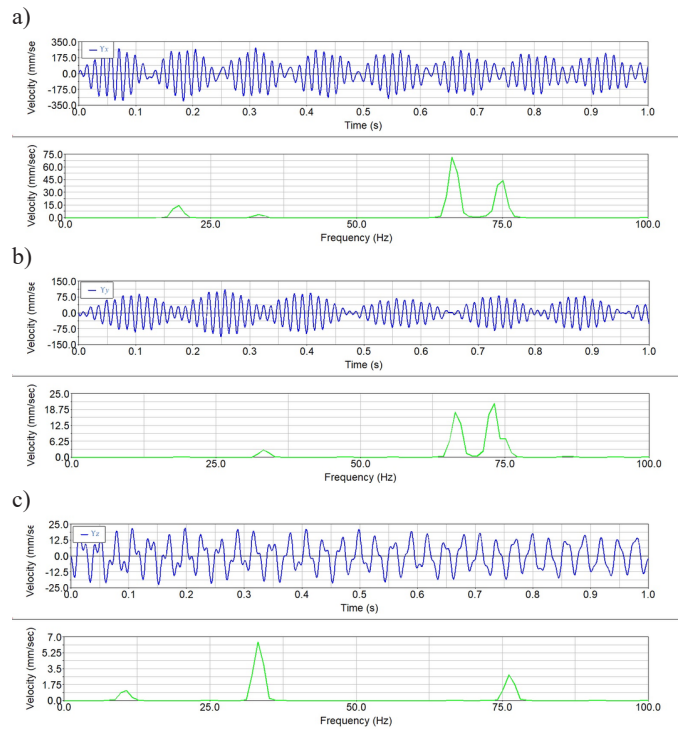


Fig. 10. Velocity response in time domain and FFT a) Y_x , b) Y_y , and c) Y_z

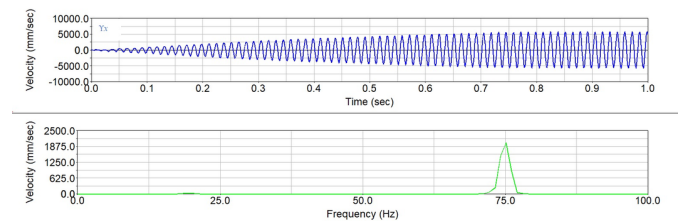


Fig. 11. Velocity response Y_x when system experiences resonance

4. Conclusion

In this study, a combination of two methods were suggested for DCR engine vibration control and monitoring; these are mechanism balancing optimization and vibrational analysis. The mathematics for system dynamics and vibration response were illustrated according to the desired sequence, where system excitation forces determination is presented and correlated to the equation of motion for vibrational analysis. Then, a balancing method was suggested using engine rotation speed variations to reduce the forces and moments caused by the DCR configuration. This method has been found to be effective because forces and moments were reduced to a marginal level, the shaking forces F_x , F_y and F_z , were reduced by 82%, 71% and 45% respectively when compared to CS balancing. Similarly, shaking moments T_x , T_y and T_z were reduced by 14%, 15% and 80% using VS balancing method.

For further verification, a vibrational study was constructed to evaluate DCR system characteristics and response. The characteristics were determined by performing a modal and frequency response analysis. The results give us basic indications about this system by identifying the system natural frequency and frequency response function, which enable us to understand safe frequency zones of balanced engine operation. Both modal and FRF give close results for system natural frequencies, where six mode shapes presented corresponding to 6 DOF.

Lastly, an analysis in time domain was conducted where the velocity response of engine COG was measured and compared to show the effect of the utilized balancing method. VS balancing method results in better velocity response when compared to common balancing method using fixed rotational speed. The results when using

VS balancing show that the velocity components Y_x , Y_y , and Y_z show less response by about 80%, 93%, and 22% respectively when compared to CS balancing. Upon implementing the effect of the optimized parameters to verify engine velocity response when running under 2000 rpm, the results show that the virtual model response was almost identical to the simulation response, the maximum difference in results between both methods was about 4% in the case of velocity component Y_z .

It can be noticed that this model can be further improved to achieve better results in terms of structure design and maintenance development. Further studies can be done considering design factors such as mounting design or by including other external excitations such as combustion pressure and internal parts friction.

References

1. Al-attab IIEKA, Zainal ZA. Alignment and Vibration Responses of High-Speed Alternator Couplings on Micro Gas Turbine. *Arabian Journal for Science and Engineering* 2020, <https://doi.org/10.1007/s13369-020-04389-7>.
2. Albaghdadi AM, Baharom MB, Sulaiman SA. Tri-planar balancing optimization of a double crank rocker mechanism for shaking forces and shaking moments reduction. *Proceedings of the Estonian Academy of Sciences* 2021; 70(3): 286-296, <https://doi.org/10.3176/proc.2021.3.07>.
3. Białas K, Buchacz A. Active reduction of vibration of mechatronic systems. *Eksplotacja i Niezawodność - Maintenance and Reliability* 2015; 17(4): 528-534, <https://doi.org/10.17531/ein.2015.4.7>.
4. Briot S, Arakelian V. Complete shaking force and shaking moment balancing of in-line four-bar linkages by adding a class-two RRR or RRP Assur group. *Mechanism and Machine Theory* 2012; 57: 13-26, <https://doi.org/10.1016/j.mechmachtheory.2012.06.004>.
5. Castilla-Gutiérrez J, Fortes J C, Pulido-Calvo I. Analysis, evaluation and monitoring of the characteristic frequencies of pneumatic drive unit and its bearing through their corresponding frequency spectra and spectral density. *Eksplotacja i Niezawodność - Maintenance and Reliability* 2019; 21(4): 585-591, <https://doi.org/10.17531/ein.2019.4.7>.
6. Delvecchio S, Bonfiglio P, Pompili F. Vibro-acoustic condition monitoring of Internal Combustion Engines: A critical review of existing techniques. *Mechanical Systems and Signal Processing* 2018; 99: 661-683, <https://doi.org/10.1016/j.ymsp.2017.06.033>.
7. Guan N, Wang A, Gu Y et al. A novel coaxial balance mechanism for reciprocating piston engines. *Applied Sciences* 2021, <https://doi.org/10.3390/app11125647>.
8. Hmida A, Hammami A, Chaari F et al. Effects of misfire on the dynamic behavior of gasoline Engine Crankshafts. *Engineering Failure Analysis* 2021; 121: 105149, <https://doi.org/10.1016/j.engfailanal.2020.105149>.
9. Hong D, Kim B. Vibration reduction against modulated excitation using multichannel NLMS algorithm for a structure with three active paths between plates. *Journal of Mechanical Science and Technology* 2019; 33(10): 4673-4680, <https://doi.org/10.1007/s12206-019-0910-0>.
10. Liu S, Li W, Shuai Z, Chen M. Vibration analysis of a single-cylinder reciprocating compressor considering the coupling effects of torsional vibration. *Shock and Vibration* 2019, <https://doi.org/10.1155/2019/3904595>.
11. Mahdisoozani H, Mohsenizadeh M, Bahiraei M et al. Performance enhancement of internal combustion engines through vibration control: State of the art and challenges. *Applied Sciences* 2019, <https://doi.org/10.3390/app9030406>.
12. Mohammed SEE, Baharom MBB, Aziz ARA. Estimation of counterweight for shaking force balancing of a crank-rocker mechanism. *Applied Mechanics and Materials* 2014; 663: 135-140, <https://doi.org/10.4028/www.scientific.net/AMM.663.135>.
13. Mohammed SE, Baharom MB, Aziz ARA. Performance and combustion characteristics of a novel crank-rocker engine. *Journal of Mechanical Science and Technology* 2017; 31(7): 3563-3571, <https://doi.org/10.1007/s12206-017-0643-x>.
14. Ooi LE, Ripin ZM. Optimization of an engine mounting system with consideration of frequency-dependent stiffness and loss factor. *JVC/ Journal of Vibration and Control* 2016; 22(10): 2406-2419, <https://doi.org/10.1177/1077546314547532>.
15. Peplow A, Isavand J, Kasaei A et al. A speed-variant balancing method for flexible rotary machines based on acoustic responses. *Sustainability* 2021; 13(13): 1-19, <https://doi.org/10.3390/su13137237>.
16. Slesongsom S, Bureerat S. Vibration suppression of a single-cylinder engine by means of multi-objective evolutionary optimisation. *Sustainability* 2018; 10(6): 2067, <https://doi.org/10.3390/su10062067>.
17. Stone R, Ball J K. *Automotive Engineering Fundamentals*. Warrendale, SAE International: 2004, <https://doi.org/10.4271/R-199>.
18. Wang D, Jiang M, He K et al. Study on vibration suppression method of vehicle with engine start-stop and automatic start-stop. *Mechanical Systems and Signal Processing* 2020; 142: 106783, <https://doi.org/10.1016/j.ymsp.2020.106783>.
19. Xu C, Cao F. Engine Excitation Force Identification on the Basis of Discrete Spectrum Correction. *Mathematical Problems in Engineering* 2015, <https://doi.org/10.1155/2015/175257>.
20. Xu Y, Huang B, Yun Y et al. Model based IAS analysis for fault detection and diagnosis of IC engine powertrains. *Energies* 2020, <https://doi.org/10.3390/en13030565>.
21. Zhang B, Zhan H, Gu Y. A general approach to tune the vibration properties of the mounting system in the high-speed and heavy-duty engine. *JVC/ Journal of Vibration and Control* 2016; 22(1): 247-257, <https://doi.org/10.1177/1077546314528963>.
22. Zhao X, Cheng Y, Wang L, Ji S. Real time identification of the internal combustion engine combustion parameters based on the vibration velocity signal. *Journal of Sound and Vibration* 2017; 390: 205-217, <https://doi.org/10.1016/j.jsv.2016.11.013>.
23. Zhao X, Yang Z, Pan B et al. Analysis of excitation source characteristics and their contribution in a 2-cylinder diesel engine. *Measurement* 2021; 176: 109195, <https://doi.org/10.1016/j.measurement.2021.109195>.